Birefringent properties of the cornea measured by a Mueller type polarimeter in healthy adults and children

Marcelina Sobczak[*] ⓘ and Magdalena Asejczyk ⓘ

Department of Optics and Photonics, Wrocław University of Science and Technology, Wybrzeże Stanisława Wyspiańskiego 27, 50-370 Wrocław, Poland
[*]*marcelina.sobczak@pwr.edu.pl*

Abstract: Mueller type polarimeter was used for *in vivo* measurements of the anisotropic parameters (retardation and azimuth angle) of corneas. To determine birefringence, corneal thickness was measured with a Scheimpflug camera (Corvist ST). The retardation distributions in the nasal-temporal cross-section in both children (N=7) and adults (N=38) groups occurred asymmetrical. The asymmetry in birefringence distributions was observed only in adults group. The geometrical analysis of the first order isochromes in both age groups showed the asymmetry of its shapes. The changes of symmetry in birefringent properties with age may have potential relationship with changing corneal biometry.

1. Introduction

The phenomenon of birefringence was discovered in 1669 by Rasmus Bartholin [1] in Iceland spar, but only in 1815 did sir David Brewster first suggest that the cornea may manifest anisotropic properties [2]. Although in 1871 Alexander Rollet suggested that anisotropic properties of the cornea are directly connected to the corneal structure, at that time this hypothesis was denied due to a lack of anatomical confirmation. However, the subsequent research suggests a connection between corneal birefringence and its structure. The thickest layer of the cornea is the stroma, which at the same time shows the greatest anisotropic properties. The corneal stroma consists of 300-500 layers of lamellas stored at random angles to each other, whereas each lamella consists of a bunch of collagen fibers, called fibrils, submerged in the ground substance. In one lamella, the collagen fibrils are arranged in parallel. Due to this specific fibrils organization in lamellas, the form birefringence is observed. In turn, a stack type organization of the lamellas in the stroma induces the resultant birefringence with complicated distribution. Preferential orientation of the lamellas' arrangement in the stroma has been presented in many models over the years [3–9].

Initially Kokott [3] presented corneal model lamellas in external stroma show vertical orientation, in midstroma are oriented towards rectus muscles attachments, but in its internal part lamellas have elliptical orientation which change to more symmetrical in the limbus area. Maurice [4] stated that there are additional lamellas in the limbus area. Daxer and Fratzl [5] presented a model where lamellas are predominately orthogonal to each other. Newton and Meek [6] modified this model noticing that fibrils orientation is changing to a radial type in the limbus area. In 2004 Aghamohammadzadeh et al. [7] reported that in the limbal area there are also additional distinguished fibril with a curved orientation or tangent to corneal limbus. In 2006 Boote et al. [8] distinguished lamellar orientation in the left and right eye and stated that in some sense they are specular reflections to one another, and the symmetry axis is placed in the sagittal plane (passing through the nose). In 2011 Boote et al. [9] complemented the model with additional limbal lamellas.

Naylor [10,11] stated that corneal birefringence is the lowest in the central part and increases parabolically to the limbus, which was later confirmed by Wang et al. [12]. Bour and Lopez

Cardozo [13] found in the *in vivo* experiment that optical path difference is equal to zero in the center and increases to the limbus. Van Blokland and Verhelst [14], also providing *in vivo* measurements, stated that the central cornea behaves like linear birefringent biaxial medium. Bueno and Vargas-Martín [15] measured paracentral and peripheral parts of the cornea and showed that the azimuth angle is constant and the optical phase difference arises from the center to the limbus, but in the paracentral part the growth is relatively small. They concluded that the cornea is a uniaxial linear birefringent medium. They noticed symmetry in isochrome shapes between the left and right eye. Hitzenberger et al. and Götzinger et al. [16,17] used PS-OCT to measure stromal anisotropy and showed that retardation increases toward the limbus and with depth.

Knighton et al. [18] used laser scanning polarimetry and described corneal anisotropy by three models. The first model assumed that the cornea is a biaxial linear birefringent medium located between two spherical surfaces, and the directions of the slow axis is nasally downward. In the second model, the slow axis is located almost completely horizontally, and one of the binormal axes is located in the pupil area. The last model assumed that the cornea is like a uniaxial linear birefringent crystal with optical axes perpendicular to the corneal surface. They stated that birefringence distribution differs for each subject. Fanjul-Velez et al. [19,20] using PS-OCT described the corneal center as a biaxial linear birefringent crystal and birefringence in its paracentral area is high and of a quasi-radial type. Bueno [21], using double-pass imaging polarimetry and Stokes-Mueller formalism, concluded that slow axis is oriented nasally downward and retardation distribution is changing between subjects. He also noticed no significant correlation between birefringent parameters and age. Mastropasqua et al. [22] used a LUMAXIS device to measure anisotropic properties of the cornea. They proposed two models: the first – a biaxial linear birefringent equivalent medium, and the second, a uniaxial linear birefringent medium. They did not rule out that the medium may be biaxial but the angle between binormal axes is small. They also noted enantiomorphism between eyes in one subject. Beer et al. [23] presented retardation distribution and its value is low in paracentral area and increases rapidly in the peripheral area. This distribution is directly connected with the lamellar structure in the stroma. However, the current knowledge is still insufficient to precisely define the structural, and thus optical, properties of the cornea. This is due to the complex structure of the cornea and its nonuniformity. Optical–polarization methods for imaging the eye microstructure are intensively developed and are increasingly used in ophthalmology.

In our previous publications [24,25], a set up for *in vivo* measurements of the corneal birefringence properties, mainly corneal retardation, has been described. The aim of this study was to correlate the Mueller-type polarimeter measurements with the corneal thickness measurements in order to determine the nature of the distribution of corneal birefringence in both age groups. The distributions of retardance, birefringence and corneal thickness were analyzed.

2. Methods

2.1. Instrumentation

A setup for measurements of birefringent properties of a living human eye was carried out in double-pass reflection mode. In this setup, it is crucial to control the polarization state of the incident beam and to measure the polarization state of the light after passing twice through the cornea. A Mueller-type polarimeter has been used, described in detail in Sobczak et al. [24,25]. In this polarimeter, the incident beam and the beam leaving the optical system mainly goes through the same way. Six images for the respective six polarimeters were recorded by the camera and analyzed (see details in [24,25]). The results enable the calculation of azimuth angle (α) and phase difference (γ) distributions of the cornea only in a limited range: for α it is [0°, 45°] and for γ [0°, 90°]. These limits are due to the usage of Mueller matrix notation. In all calculation it is assumed that the human cornea can be treated as a non-dichroic, linear

birefringent medium. Additionally, to calculate birefringence of the cornea in a horizontal cross section (nasal-temporal cross section), the corneas thickness (CT) was measured using Corvis ST with Scheimpflug camera (OCULUS Optikgeräte GmbH; Wetzlar, Germany).

2.2. Samples

Forty-five healthy Caucassian volunteers (aged 10-59) were recruited for this study. The subjects were divided into two age groups: seven children (10-15 years old) and thirty eight adults (26-59 years old). The volunteers have no refractive errors, or they were negligible (spherical equivalent was maximum 2.0 D). The measurements were conducted and analyzed for both left and right eyes for each subject, and each eye was measured three times. The measurement procedure started with the right eye, where the measured cornea was evenly illuminated, and the subject looked straight at the light stimulus (placed at the 5 m distance) without blinking for about 6 seconds. The measurements of the birefringent parameters were carried out in darkness; the only light came from a completely polarized optical system. The measurements of all subjects were performed when their iris was a natural size.

The project was approved by the Ethics Committee of Wroclaw Medical University (KB 329/2014) and adhered to the tenets of the Declaration of Helsinki. The adult participants and children with their legal guardians were fully informed of their requirements, as well as the purpose and procedures of the study. Informed parental consent and the adult participants assent were obtained before measurements were taken. Study exclusion criteria included any systemic disease, history of ocular trauma or eye disease, refractive surgery less than 6 months before the study start date, conjunctival or intraocular inflammation, or corneal abnormalities.

2.3. Data analysis

Obtained from the measurements, images of the cornea and background underwent the image processing procedure (described in detail in Sobczak et al. [25]). The procedure yielded distribution maps of α and γ (see Fig. 1).
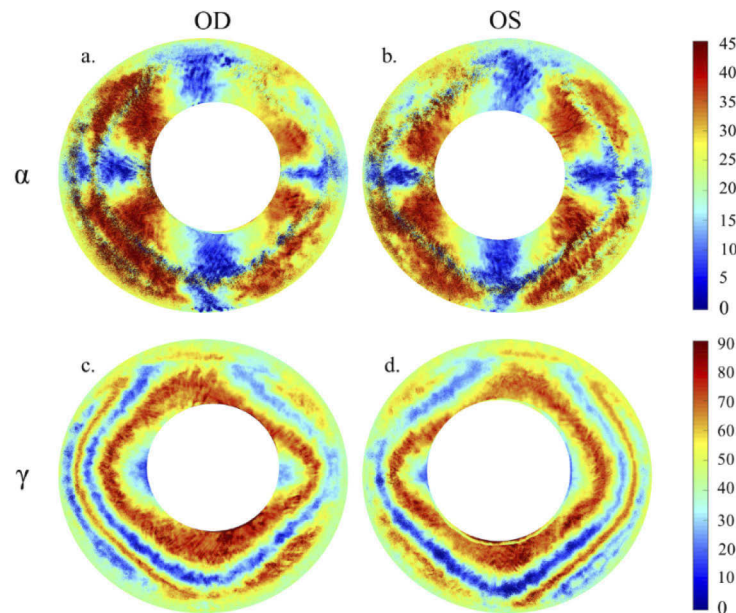
Fig. 1. Exemplary results of experimental distribution of α (a, b) and γ (c, d). Left column (a, c) stands for the right eye and right column (b, d) for the left eye

From the distribution maps of α three distributions for different distances from the corneal apex were designated: 25%, 50% and 75% of half width of the image (Fig. 2). To do this, it was necessary to transform the image from spherical coordinates $(\alpha[r(x, y), \alpha_{lab}(x, y)])$ to cartesian ones $(\alpha(r, \alpha_{lab}))$, and the line along which the transformation starts corresponds to the zero line on the TABO scale, known as conformal mapping. Due to the limitations of the results, it was necessary to perform the unwrapping procedure for distributions of α. The last step of the azimuth angle analysis was to approximate the reconstructed distribution with a linear function described as $\alpha = \alpha_{lab} + b$, where α_{lab} – the cross-section angle in the laboratory coordinate system.
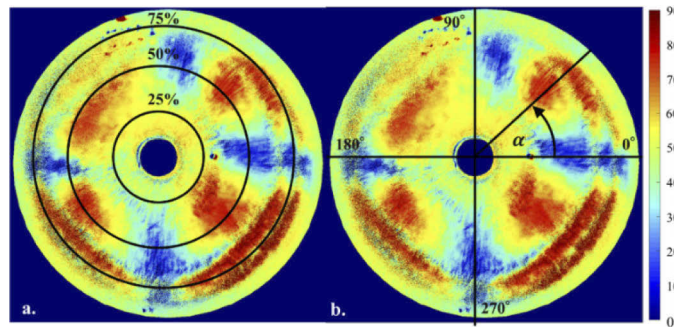

Fig. 2. Distribution of α: scheme of the radial representation of this distribution (a), scheme of tangential representation for three selected circles (b)

The analysis of the γ was as follows: first, on its distribution maps, the inflection points of the first isochrome were appointed (white dots in Fig. 3), then based on these coordinates lengths of the sides (B_{TU}, B_{TD}, B_{NU}, B_{ND}), angles between these sides (α_N, α_T, α_U, α_D) and lines: 0 – passing through two "horizontal" dots, 90 – passing through two "vertical" dots, +45 and −45 – were designated as bisectors of the angles formed from the intersection of lines 0 and 90 (black lines Fig. 3). Through all these lines the distribution of γ was determined. Each of these distributions was divided into two parts. The point of division was the point of intersection of all designated lines. Due to the limitations of the results, it was necessary to perform the unwrapping procedure for γ. The reconstructed distributions were approximated by fourth degree shifted Chebyshev polynomials. The polynomials are orthogonal, which enable the performance of a statistical analysis of polynomial coefficients.

Analogical analysis was performed for the horizontal cross-section of the distributions passing through coordinates of the corneal apex. The distributions of corneal thickness (CT) were received for the same cross-section (horizontal cross section) using CORVIS ST (Scheimpflug camera). It allowed calculation of the absolute value of birefringence in each point of the distribution. From the optical point of view, birefringence (Δn) is defined as the ratio of the retardation (R) and optical path (d). On the other hand γ is proportional to R: $\gamma = 2\pi R/\lambda$, where λ is the wavelength of the light used in an experiment. For the purpose of this study, the optical path was assumed to be equal to the thickness of the cornea. The distributions of birefringence were approximated also by fourth degree shifted Chebyshev polynomials.

A reproducibility analysis of the parameters was performed to check whether a single measurement of the eye parameters is sufficient and reliable. Images for both left and right eyes were taken ten times, and their similarity tested using Matlab scripts. Errors of designation of side lengths and angles were estimated sequentially for 10 px and 1°. The calculated standard deviations for both parameters appeared to be lower. Theirs coefficients of variation (CV) are below 1%. Pearson correlation coefficients for each α distribution were high >0.97, $p<0.001$, as well as for each γ distribution (>0.946), $p<0.001$, and for each birefringence distribution
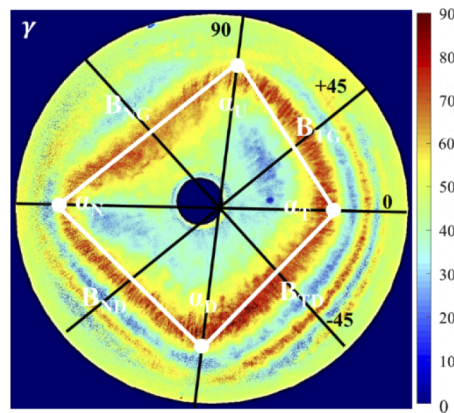
Fig. 3. Distribution of γ described by a quadrilateral (sides lengths: B_{NU}, B_{ND}, B_{TU}, B_{TD}, vertex angles α_N, α_T, α_U, α_D) with marked lines of cross-sections (0, 90, +45, −45)

in horizontal cross-section 0.999, $p<0.001$, which confirmed high reproducibility of these parameters.

Statistical analysis was performed using Statistica (TIBCO Software). The analyses were preceded with testing for data normality (Shapiro-Wilk test). The Shapiro-Wilk test did not reject the hypothesis of data normality of corneal thickness (CT). A T-test was applied for the CT as it was compared between the central and paracentral areas and between the right and left eye. A non-parametrical Wilcoxon rank-sum test was used to compare the median of geometrical parameters of the conoscopic figures: side length (B_{TU}, B_{TD}, B_{NU}, B_{ND}) and the vertex angles (α_N, α_T, α_U, α_D) between them. Distributions of the azimuth angle α was approximated by the linear function. The difference between distributions for the left and right eye was tested using a Fisher test. To test whether retardation (R) distributions described by Chebyshev polynomials was different from each, the assumption was made that if all pairs of the coefficients of respective polynomials were statistically different (Wilcoxon test), these two polynomials, and hence their distributions, were different. Otherwise the hypothesis was rejected. The same procedures was conducted for calculated birefringence. The significance level for all the tests was set to $p=0.05$.

3. Results

3.1. Corneal thickness analysis

Mean values (±SD) of corneal thickness in both group of children and adults are: in the central part (CCT; for adults 545 ± 26, for children 566 ± 31) and paracentral part (PCT) (PCT_N – nasal, PCT_T – temporal) of the cornea for two distances from corneal apex – 3.5 mm (for adults $PCT_N=664 \pm 34$, $PCT_T=621 \pm 36$, and for children $PCT_N=695 \pm 37$, $PCT_T=638 \pm 41$) and 4.0 mm (for adults $PCT_N=700 \pm 40$, $PCT_T=6648 \pm 41$, and for children $PCT_N=735 \pm 40$, $PCT_T=665 \pm 45$).

Distribution (box-plots) of CT are presented in Fig. 4 for the older age group (Fig. 4(a)) and the younger age group (Fig. 4(b)). The highest value of the corneal thickness in both age groups was found in the nasal part of the horizontal cross-section of the cornea.

There was no significant difference between right and left eyes in all appointed corneal thicknesses in both age groups ($p>0.05$). However, when these parameters were compared in age groups, there were statistically significant differences in the nasal part of the cornea (PCT_N) in 4.0 mm and 3.5 mm (t-Student test, $p=0.003$ and $p=0.004$, respectively) and in central corneal thickness CCT ($p=0.009$). Comparing corneal thickness between different points of the cornea,
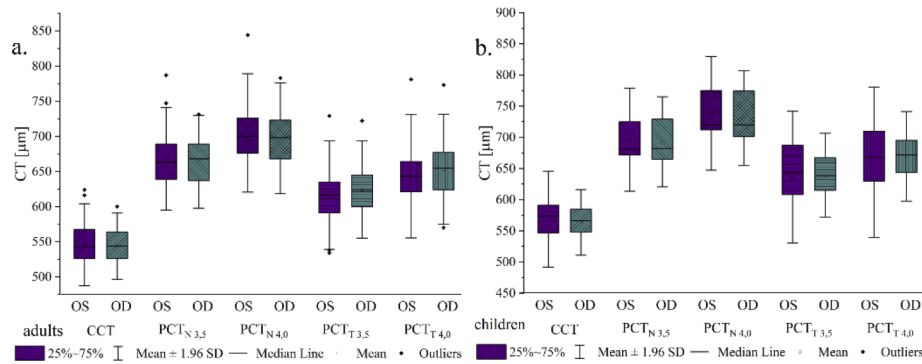
Fig. 4. Box-plots of corneal thickness (CT) for adult (a) and children (b) groups in central area *CCT*, and nasal and temporal paracentral area measured in 3.5 mm and 4.0 mm ($PCT_{N\ 3,5}$, $PCT_{N\ 4,0}$, $PCT_{S\ 3,5}$, $PCT_{S\ 4,0}$, respectively)

significant differences were denoted for both the older and younger age group (t-Student test, $p<0.001$).

3.2. Geometrical analysis of birefringence patterns

The mean values of side lengths (B_{TU}, B_{TD}, B_{NU}, B_{ND}) and quadrangle angles between them (α_T, α_N, α_U, α_D), representing the first isochrome for both age groups divided into the left (OS) and right (OD) eye, are presented in Fig. 5. In both age groups the longest calculated side was B_{NU} both in the left and right eyes (Fig. 5(a, (b))). The shortest side in OS and OD eyes for both age groups was B_{TD}. In the adult group three of four side lengths (B_{TD}, B_{NU}, B_{ND}) were significantly different between the left and right eye (respectively $p=0.029$, $p<0.001$, $p=0.031$). The biggest angle in both eyes for the adult group was noticed in the temporal part of the cornea α_T, and the smallest, in the nasal part α_N (Fig. 5(c, (d))). In this age group the significant statistical difference in angle value between the two eyes occurred only in the superior part of the cornea α_U ($p=0.018$). Looking at the results for the younger age group, the highest value of the designated angles was in the inferior part of the cornea, and the lowest, in the nasal part. None of the angle values were significantly different between the left and right eye ($p<0.10$).

The dependences between the above-mentioned geometrical parameters were also checked in both eyes for both age groups (Table 1). There were significant statistical differences ($p<0.050$, Wilcoxon test) between most of the side pairs (B_{TU} vs. B_{TD}, B_{TU} vs. B_{NU}, B_{TD} vs. B_{NU}) in both age groups. There were no significant differences in all groups between B_{TD} and B_{ND} ($p>0.100$), and in the children's group, in right eye between B_{TU} vs. B_{ND} ($p=0.063$). Considering the comparison between vertex angles, there were significant difference between α_T vs. α_N, α_N vs. α_U, and between α_N vs. α_D in both eyes and age groups. In three of four cases there was no relevant difference between α_T and α_D, except for the right eye in the children's group (Wilcoxon test, $p=0.042$). Between α_T vs. α_U and α_U vs. α_D there was significant difference in the adult group in both eyes, while there was no relevant difference in the children's group.

When the results were not distinct for the left and right eye, there was no significant difference in both age groups between B_{TD} vs. B_{ND} (Table 2). There were relevant differences between α_T vs. α_U and α_U vs. α_D only for the adult group, while the same relationships were not statistically significant in the children's group.

3.3. Analysis of the anisotropic parameters

Determination coefficients R^2 of approximation of α distribution at three different distances from the corneal apex (25%, 50% and 75% of half width of the image) are appointed. For the
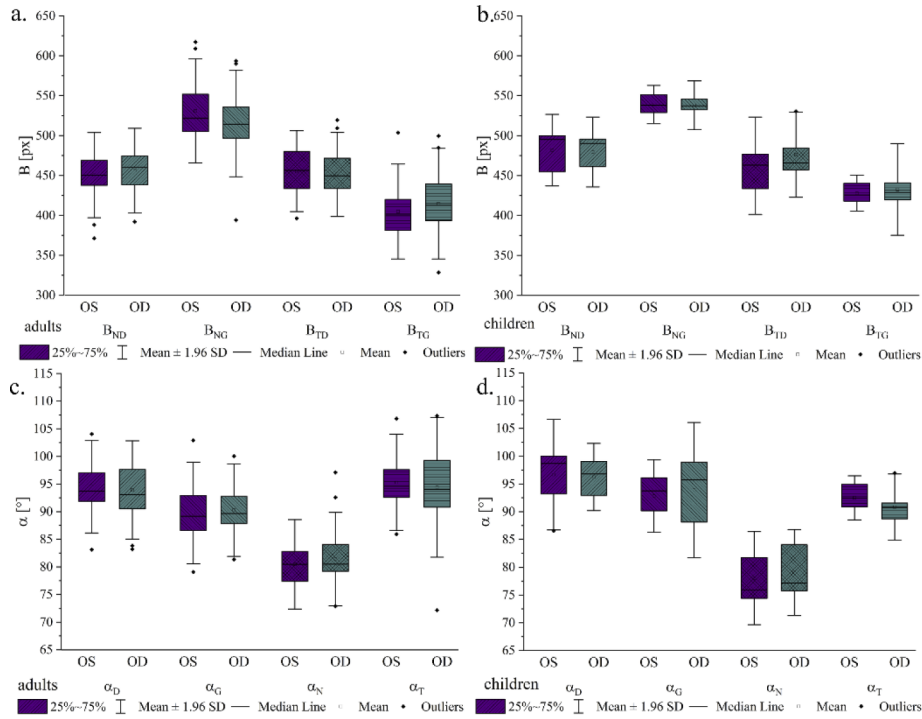
Fig. 5. Box-plots of sides lengths (B_{SG}, B_{NG}, B_{ND}, B_{SD}) (a, b) and angles sizes between them (α_T, α_U, α_N, α_D) (c, d) for right and left eye in both age groups

Table 1. Results of Wilcoxon test (p-value) for dependencies between sides' pairs and angles' pairs for two age groups: adults and children for right OD and left OS eyes[a]

	p-value					*p*-value			
	adults		children			adults		children	
	OD	OS	OD	OS		OD	OS	OD	OS
B_{TU} vs. B_{TD}	**<0.001**	**<0.001**	**0.043**	**0.028**	α_T vs. α_N	**<0.001**	**<0.001**	**0.018**	**0.018**
B_{TU} vs. B_{NU}	**<0.001**	**<0.001**	**0.018**	**0.018**	α_T vs. α_U	**0.018**	**<0.001**	0.310	0.735
B_{TU} vs. B_{ND}	**<0.001**	**<0.001**	0.063	**0.018**	α_T vs. α_D	0.744	0.446	**0.042**	0.237
B_{TD} vs. B_{NU}	**<0.001**	**<0.001**	**0.043**	**0.028**	α_N vs. α_U	**<0.001**	**<0.001**	**0.018**	**0.018**
B_{TD} vs. B_{ND}	0.194	0.607	0.735	0.176	α_N vs. α_D	**<0.001**	**<0.001**	**0.018**	**0.018**
B_{NU} vs. B_{ND}	**<0.001**	**<0.001**	**0.018**	**0.018**	α_U vs. α_D	**0.018**	**<0.001**	0.310	0.128

[a]bold denotes statistical significance

adult group this coefficient ranged from 0.965 to 0.997 (*p*<0.001), and in the children's group, 0.863-0.993 (*p*<0.001). For each distribution there was a significant statistical difference between age groups (Fisher test, *p*<0.005).

Figure 6 presents exemplary distributions of retardation (Fig. 6(a, c, e)) and birefringence (Δn) (Fig. 6(b, d, f)) for the adult group (Fig. 6(a-d)) and children's group (Fig. 6(e, f)). In most cases differences between R values in the horizontal temporal cross-section and horizontal nasal cross-section were noticed. In most cases differences between values in the horizontal temporal cross-section and horizontal nasal cross-section were noticed.

Distributions of R were approximated by fourth degree Chebyshev polynomials. Determination coefficients R^2 ranged from 0.624 to 0.999 (*p*<0.001). In the adult group the lowest values of R^2

Table 2. Results of Wilcoxon test (p-value) for dependencies between sides' pairs and angles' pairs for two age groups: adults and children[a]

	p-value				*p*-value	
	adults	children			adults	children
B_{TU} vs. B_{TD}	**<0.001**	**0.004**	α_T vs. α_N		**<0.001**	**0.001**
B_{TU} vs. B_{NU}	**<0.001**	**0.001**	α_T vs. α_U		**<0.001**	0.300
B_{TU} vs. B_{ND}	**<0.001**	**0.002**	α_T vs. α_D		0.437	**0.019**
B_{TD} vs. B_{NU}	**<0.001**	**0.001**	α_N vs. α_U		**<0.001**	**0.001**
B_{TD} vs. B_{ND}	0.572	0.198	α_N vs. α_D		**<0.001**	**0.001**
B_{NU} vs. B_{ND}	**<0.001**	**0.001**	α_U vs. α_D		**<0.001**	0.084
B_{TU} vs. B_{TD}	**<0.001**	**0.004**	α_T vs. α_N		**<0.001**	**0.001**

[a]bold denotes significant statistical difference
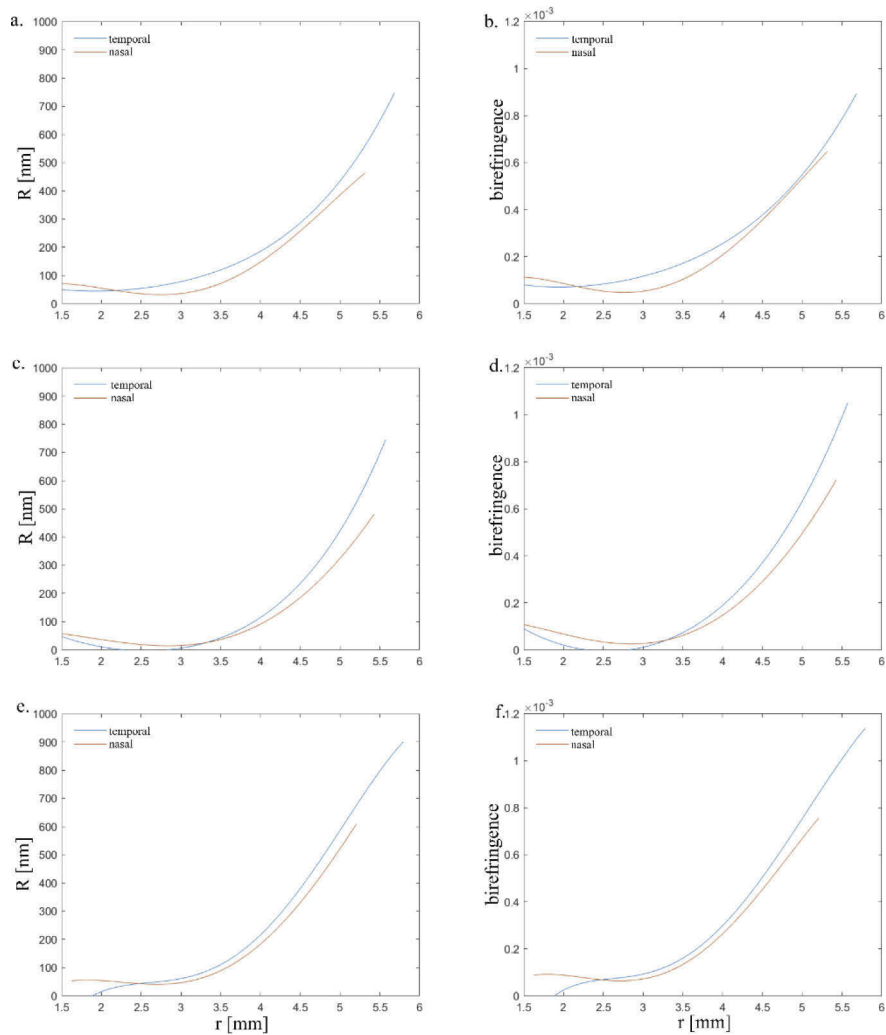
Fig. 6. Examples of retardation (R) (a, c, e) and birefringence (Δn) (b, d, f) distributions for adults (a-d) and children (e, f)

Table 3. Wilcoxon test (p-value) for Chebyshev polynomials' coefficients for retardance R distributions[a]

	i	j	a_{0i} vs. a_{0j}	a_{1i} vs. a_{1j}	a_{2i} vs. a_{2j}	a_{3i} vs. a_{3j}	a_{4i} vs. a_{4j}
adults	T	N	**<0.001**	**0.003**	**<0.001**	**<0.001**	**<0.001**
	U	D	0.095	**0.011**	0.123	**0.012**	0.154
	TU	ND	0.991	0.870	0.950	0.941	0.537
	TD	NU	**0.020**	**0.014**	**0.010**	**0.004**	**0.010**
	TU	TD	**0.006**	**0.002**	**0.003**	**0.001**	**0.005**
	NU	ND	0.764	0.963	0.812	0.872	0.686
	T	U	**0.005**	0.091	**0.012**	**0.014**	**0.029**
	T	D	0.255	0.059	0.332	0.334	0.416
	N	U	0.810	0.874	0.630	0.520	0.206
	N	D	**<0.001**	**<0.001**	**<0.001**	**<0.001**	**0.022**
children	T	N	**0.001**	**0.001**	**0.001**	**0.001**	**0.002**
	U	D	0.683	0.551	0.683	0.777	0.730
	TU	ND	0.470	0.638	0.397	0.683	0.683
	TD	NU	0.730	0.073	0.594	0.056	0.470
	TU	TD	**0.048**	**0.030**	**0.030**	**0.019**	**0.041**
	NU	ND	0.124	0.245	0.158	0.221	0.330
	T	U	**0.011**	**0.015**	**0.011**	**0.008**	**0.003**
	T	D	**0.019**	0.177	**0.013**	**0.048**	**0.005**
	N	U	0.300	0.245	0.551	0.300	0.594
	N	D	0.433	0.096	0.925	0.096	0.470

[a]T – temporal, N – nasal, U – upper, D – down, TU – temporal upper, TD – temporal down, NU – nasal upper, ND – nasal down, bold denotes statistical significance

were in the nasal superior cross-section of the cornea (R^2=0.624÷0.998), while the highest, in the temporal inferior (R^2=0.949÷0.999). In the children's group the determination coefficient R^2 ranged from 0.919 to 0.997 ($p<0.001$).

In order to determine whether the distributions of the retardance (R) are different from each other in the considered cross-sections, the differences between the polynomial coefficients (a_{ki} vs. a_{kj}, k=0-4) were tested with a Wilcoxon test ($p<0.050$) (Table 3). In the adult group significant differences appeared between distributions in temporal (T) and nasal (N) cross-sections, between temporal down (TD) and nasal upper (NU) cross-sections, between temporal upper (TU) and temporal down (TD), and between nasal (N) and down (D) cross-sections of the corneal paracentral area (Table 7). In the children's group significant differences were for pairs of cross-sections: nasal (N) and temporal (T), temporal down (TD) and temporal upper (TU), and temporal (T) and upper (U).

Birefringence (Δn) distributions (Fig. 6(b,d,f)) were approximated with fourth degree Chebyshev polynomials for all approximations $R^2 \sim 0.999$ ($p<0.001$). In order to compare the distributions in the horizontal cross-section (nasal and temporal ones), the same statistical hypothesis was stated for comparison of R. In the group of adults the birefringence distributions were different (Wilcoxon test, $p<0.001$), while in the children's group those differences did not appear ($p>0.100$) (Table 4).

Table 4. Results of Wilcoxon test (p-value) for coefficients' pairs of Chebyshev polynomials for horizontal birefringence (Δn) distribution in nasal and temporal part of the cornea for both age groups[a]

	p-value	
	adults	children
a_{0T} vs. a_{0N}	**<0.001**	0.116
a_{1T} vs. a_{1N}	**<0.001**	0.116
a_{2T} vs. a_{2N}	**<0.001**	0.133
a_{3T} vs. a_{3N}	**<0.001**	0.116
a_{4T} vs. a_{4N}	**<0.001**	0.173

[a]bold denotes statistical significance

4. Discussion

The corneal birefringence comes from anisotropy of the lamellas and their arrangement in the stroma [16,26–28]. Profound knowledge of the corneal anisotropy is the key to determining the microstructure of the cornea, but also to understanding how ophthalmic and systemic diseases affect its structure. The measurement setup used in this experiment was a double-pass Mueller-type polarimeter [24,25]. Usage of this type of polarimeter allows us to acknowledge that the human cornea is a non-dichroic medium, because the gained light intensity distributions (taken from polarimeter) are, in pairs, the same: the first obtained with horizontal and vertical linear polarimeters, the second, with left-skewed and right-skewed linear polarimeters, and the third, with right-handed and left-handed circular polariscopes. But the utilization of this optical system imposes a restriction to the measurement method in the received results. For the azimuth angle (α) it is [0°, 45°], while for the phase difference (γ) it is [0°, 90°], which is why it was necessary to apply the unwrapping of the received distributions.

The geometrical parameters of the first order isochrome - the length of the sides of the describing polygon (B_{TU}, B_{TD}, B_{NU}, B_{ND}) and the angles of the vertices between them (α_N, α_T, α_U, α_D) - were extracted from first order isochromes of a given eye. Statistical analysis showed that there is a mirror symmetry of first order isochromes between the left and right eye in one subject. Considering the angles of the first isochrome quadrangle, it should be noted that the significant differences appeared between the nasal and temporal angles. It confirmed our previously reported results [29], using biomicroscope with a circular polarizer to measure the geometrical parameters of the first and second order conoscopic figures. The asymmetry in shape of the first order conoscopic figures was shown, while the second fringe in the children's group appeared to be more symmetrical than in the adult group.

In this paper, we analyzed geometrical parameters of the first order isochromes, and asymmetry in both age groups was obtained. The asymmetry of the conoscopic figure/isochrome shape could be caused by asymmetry in corneal thickness. It is seen in both younger and older groups, although in the first group the asymmetry around the limbal area is lower, which may have been caused by a changing corneal thickness with age. The results for corneal thickness showed no difference between the left and right eye, while they showed relevant difference between paracentral corneal thickness in the nasal and temporal part of the cornea. There was a significant statistical difference between the two age groups only for central corneal thickness and nasal paracentral corneal thickness. In Sobczak et al. [29] the difference was indicated in central, paracentral temporal and paracentral nasal corneal thicknesses between age groups. This different result may be due to a small sample size in the children's group in our experiments. Rüfer et al.

[30] noted that there was significant change in peripheral corneal thickness in the nasal part of the cornea with age, while it was not noticed in the temporal area of the cornea.

Taking into account that the inflection points of the designated polygons are overlapping with rectus extraocular muscles attachments, it might be supposed that these muscle forces participate in the distribution of corneal birefringence. The forces of superior rectus and inferior rectus are alike, but there is a great disproportion between forces of medial rectus and lateral rectus in favor of medial [23]. Boote et al. [31] suggested that asymmetry in lamella distribution, also birefringence distribution, may be caused by the forces of extraocular muscles. They showed that the density of the lamellas are greater in limbus and sclera in four cardinal points directed towards the attachments of the rectus extraocular muscles. The results of the measurements using stress tomography have shown that lamella distributions are in favor of stress distribution for eye movements [32]. If the rectus extraocular muscles affected the formation of lamella distribution, the effect of increasing disproportion in geometrical parameters of isochromes would occur with age. While we did not observe this phenomenon, disproportion occurred in distributions defined in this article: birefringence in the adult group, while in the children's group this disproportion was not noticed.

Distributions of α, regardless of the cross-sections, showed a high linear correlation in both age groups. So, it could be stated that the distributions of α is radial, mainly in the peripheral area of the cornea. Our results showed that γ of the human cornea increase from the apex to the corneal periphery. There were also eyes whose retardation distribution in some cross-sections was not minimal at the apex. Firstly, it decreases to the minimum value and then increases towards the limbus. This discrepancy may be due to the varying angle between binormal axes if assumed that the cornea is treated as a biaxial, linear birefringent medium, or that some corneas could be regarded as uniaxial crystals and others as biaxial ones.

It should be noted that retardance should not be equated with birefringence, especially when trying to draw conclusions about the organization of the lamellas in the cornea. This distribution directly affects the birefringence of the cornea, and in the measuring system it affects the retardation. It should be noted that a specific increase of the retardation does not indicate that birefringence behave in the same way. Retardation is a function of birefringence and a geometrical light path. Birefringence is also not one value closely related to a specific place, because it is a function of light propagation in an anisotropic medium. It means that there might be situations in which, in special light conditions (convergent/divergent light beam), birefringence distribution function will not be monotonic. In our study, the statistically relevant difference appeared between retardation distributions in nasal and temporal cross-sections in both age groups, while there was none between the top and bottom cross-section. In the adult group there were also significant differences in retardation distributions between cross-section in temporal-down and nasal-upper parts of the cornea, in temporal-upper and temporal-down, and in nasal and down corneal parts. In the children's group significant differences were between retardation distributions in temporal-down and temporal-upper parts, and in temporal and upper part of the cornea. The comparison of the birefringence distributions in the nasal and temporal corneal cross-sections shows that in the group of adults there was a significant difference between these distributions, while in children there was none found. To our knowledge there was no research about differences in retardation distributions or birefringence in particular cross-sections of the cornea in age groups. If anything, it is just the differences in birefringence or retardance values between central and paracentral corneal area were described [18,33,34]. In the literature, it is reported that the retardation/birefringence increases from the center to the limbus area. Fukuda et al. [34] using PS-OCT stated that there is no difference in corneal thickness and retardation between people in their twenties and sixties. These findings are in accordance with this study for adults 26-59 years old. Knighton et al. [18] concluded that corneal birefringence highly depends on external conditions under which the measurements were performed (e.g. divergence of light

beam). Bueno and Vargas-Martín [15] determined that the retardation value increases from the corneal apex towards the limbus, but in the paracentral and limbal area the growth is weaker. Using PS-OCT, Beer et al. [23] presented maps of retardation and optical axis orientation. They showed that in the central area of the cornea the retardation is low and it highly increases toward the limbus. Similar research was conducted by Hitzenberger et al. [16] and Götzinger et al. [17], but they additionally showed that retardation not only is changing from apex to limbus but also with stromal depth. Like us, Beer et al. [23] has also shown that the retardation distributions show a mirror symmetry between the left and right eye in each subject. Based on our measurement result, we concluded that the corneal behaves like a biaxial, non-dichroic linear birefringent medium. These findings are in accordance with reports of Fanjul-Velez et al. [19], who studied the corneas *in vivo* and *in vitro* using PS-OCT. They assumed that in the central area the cornea is a biaxial linear birefringent medium, and the limbal area is quasi-radial with high values of birefringence. Knighton et al. [18] also described the cornea as a biaxial linear birefringent medium, but they emphasized that some of the corneas behave more like uniaxial crystal, where the optic axis is perpendicular to its surface. Bueno and Vargas-Martín [15] measured the paracentral area of the cornea and stated that, in most cases, the slow optical axis is directed nasally downward.

The results obtained in our study lead to the conclusion that the asymmetry of the retardation distribution (asymmetry of the shape of the first order isochrome; see Fig. 6) is influenced not only by the asymmetry of the corneal thickness distribution, but also by the asymmetry of the birefringence distribution. It is the largest in the horizontal cross-section, and the smallest in the vertical cross-section [29]. This would mean that there is an asymmetry in the lamellar distribution. This assumption is also reflected in the literature [8]. In our research, we obtained a very interesting result that the asymmetry of birefringence in children is smaller than in adults (or even does not occur). So far this phenomenon has not been described in the literature. The reason for the lack of asymmetry in the distribution of birefringence in children may be the different organization of the lamellas, which reorganize with age. As a consequence, in adults, this organization shows greater asymmetry in the horizontal cross-section. Irsh et al. [35] examined the central corneal birefringence and found no significant correlation between the central corneal birefringence and age (in the group of people aged 3 to 70 years). Our results are consistent not only with the studies by Irsh et al. [35], but also with reports on structural changes in the central cornea with age [36,37]. Although there are significant changes in the thickness of the cornea as well as changes in its structure after birth, they last until about the sixth month of life [37]. Later they are much smaller [36]. Gogola et al. [38] analyzed changes in collagen fibrils' tortuosity in the stroma and it turned out that with age there is a significant monotonic decrease (research group from 1 to 97 years old) in the central and peripheral cornea and limbus. Corneal asymmetry is influenced also by the change in toricity with age, as indicated by the change in rule-compliant astigmatism to anti-rule astigmatism [39,40].

Since the corneal birefringence results mainly from the arrangement of collagen fibrils in the stroma, it could be a parameter supporting ophthalmic diagnostics. Some eye or corneal diseases are related to a disorder of the corneal microstructure, e.g. keratoconus. Optical methods, which have been widely developed in recent years, work best in such diagnostics. These are complex devices, such as PS-OCT, which enable the visualization of the corneal structure at the microscopic level [34,41]. Some systemic diseases, such as diabetes, can also cause structural changes to the cornea. In the course of the disease, among other things, atrophy of subepithelial nerve plexus occurs. The only known diagnostic method in these cases is confocal microscopy, but it is a method that allows examination of very small areas of the cornea. There is no method that would allow a global assessment of structural changes in the cornea. In terms of global mapping of the corneal structure, the Mueller-type double-pass polariscope appears to be a promising non-invasive method.

The results presented in this article may have an impact on ophthalmic surgery procedures, both current and developing methods. This means the development of ophthalmic transplantation, both penetrating keratoplasty and layered keratoplasty, disrupting the mechanical and structural properties of the cornea. The success of the procedure and the quality of vision depend on the correct orientation of the implant in relation to the structure of the recipient's cornea. The orientation and number of lamellas have a direct impact on the shape and number of visible isochromes. Therefore, the success of transplantation can be achieved by optimizing the position of surgical incisions and the appropriate orientation of the transplanted tissue. Future transplant methods should therefore take into account the integrity of the corneal microstructure.

5.　Conclusion

The paper describes the distributions of the azimuth angle, retardation and birefringence of the human eye cornea. This study not only confirmed the previously reported results, but also allowed for more precise determination of the nature of the birefringence phenomenon. In particular, the asymmetry of the shapes of conoscopic figures and their potential relationship with corneal biometry and age were determined.

The distributions of retardance in the horizontal cross-section (nasal-temporal cross-section) in both children and adults are asymmetrical, while in the distributions of birefringence, asymmetry is observed only in adults. The distributions of birefringence in children are symmetrical. The change of this symmetry with age may result from the changing biometry of the cornea with age in its different areas (nasal-temporal cross-section).

Disclosures. The authors declare that there are no conflicts of interest related to this article.

Data availability. Data underlying the results presented in this paper are not publicly available at this time but may be obtained from the authors upon reasonable request.

References

1. R. Bartholin, "An account of sundry experiments made and communicated by that learn'd mathematician, Dr. Erasmus Bartholin, upon a chrystal-like body, sent to him out of Island," Philos Trans R Soc. **5**, 2041–2048 (1670).
2. D. Brewster, "Experiments on the de-polarization of light as exhibited by various mineral, animal and vegetable bodies with a reference to the general principles of polarization," Philos. T. R. Soc. Lond. **105**, 21–53 (1815).
3. W. Kokott, "Uber mechanisch-funktionelle Strukturen des Auges," Graefe's Arch. Clin. Exp. Ophthalmol. **138**(4), 424–485 (1938).
4. D. M. Maurice, *The Eye: The Cornea and Sclera*, H. Davson, ed. (Academic Press, 1984).
5. A. Daxer and P. Fratzl, "Collagen fibril orientation in the human corneal stroma and its implication in keratoconus," Invest. Ophthalmol. Visual Sci. **38**(1), 121–129 (1997).
6. R. H. Newton and K. M. Meek, "The integration of the corneal and limbal fibrils in the human eye," Biophys. J. **75**(5), 2508–2512 (1998).
7. H. Aghamohammadzadeh, R. H. Newton, and K. M. Meek, "X-ray scattering used to map the preferred collagen orientation in the human cornea and limbus," Structure **12**(2), 249–256 (2004).
8. L. J. Bour, *Visual Optics and Instrumentation: Polarized Light and the Eye*, W. N. Charman and J. R. Cronly-Dillon, eds. (Macmillan Press, 1991).
9. C. Boote, C. S. Kamma-Lorger, S. Hayes, J. Harris, M. Burghammer, J. Hiller, N. J. Terrill, and K. M. Meek, "Quantification of collagen organization in the peripheral human cornea at micron-scale resolution," Biophys. J. **101**(1), 33–42 (2011).
10. E. J. Naylor, "The structure of the cornea as revealed by polarized light," J. Cell. Sci. **s3-94**(25), 83–88 (1953).
11. E. J. Naylor, "Polarized light studies of corneal structure," Br. J. Ophthalmol. **37**(2), 77–84 (1953).
12. T. J. Y. Wang and F. A. Bettelheim, "Comparative birefringence of cornea," Br. J. Ophthalmol. **51**(1), 89–94 (1975).
13. M. Dubbelman, V. A. D. P. Sicam, and G. L. van der Heijde, "The shape of the anterior and posterior surface of the aging human cornea," Vision Res. **46**(6-7), 993–1001 (2006).
14. G. J. van Blokland and S. C. Verhelst, "Corneal polarization in the living human eye explained with a biaxial model," J. Opt. Soc. Am. A **4**(1), 82–90 (1987).
15. J. M. Bueno and F. Vargas-Martín, "Measurements of the corneal birefringence with a liquid-crystal imaging polariscope," Appl. Opt. **41**(1), 116–124 (2002).
16. E. Götzinger, M. Pircher, M. Sticker, A. F. Fercher, and C. K. Hitzenberger, "Measurement and imaging of birefringent properties of the human cornea with phase-resolved, polarization-sensitive optical coherence tomography," J. Biomed. Opt. **9**(1), 94–102 (2004).

17. C. K. Hitzenberger, E. Götzinger, and M. Pircher, "Brefringence properties of the human cornea measured with polarization sensitive optical coherence tomography," Bull. Soc. Belge. Ophthalmol. **302**, 153–168 (2006).

18. R. W. Knighton, X. R. Huang, and L. A. Cavuoto, "Corneal birefringence mapped by scanning laser polarimetry," Opt. Express **16**(18), 13738–13751 (2008).

19. F. Fanjul-Veléz, M. Pircher, B. Baumann, E. Götzinger, C. K. Hitzenberger, and J. L. Arce-Diego, "Polarimetric analysis of the human cornea measured by polarization-sensitive optical coherence tomography," J. Biomed. Opt. **15**(5), 056004 (2010).

20. F. Fanjul-Vélez and J. L. Arce-Diego, "Polarimetry of birefringent biological tissues with arbitrary fibril orientation and variable incidence angle," Opt. Lett. **35**(8), 1163–1165 (2010).

21. J. M. Bueno, "Analysis of the central corneal birefringence with double-pass polarimetric images," J. Mod. Opt. **58**(19-20), 1864–1870 (2011).

22. R. Mastropasqua, M. Nubille, N. Salgari, M. Lanzini, R. Callenno, P. A. Mattei, A. Sborgia, and L. Agnifili, "Interference figures of polarimetric interferometry analysis of the human corneal stroma," PLoS One **12**(6), e0178397 (2017).

23. F. Beer, A. Wartak, R. Haindl, M. Gröschl, B. Baumann, M. Pircher M, and C. K. Hitzenberger, "Conical scan pattern for enhanced visualization of the human cornea using polarization sensitive OCT," Biomed. Opt. Express **8**(6), 2906–2923 (2017).

24. M. Sobczak, P. Kurzynowski, W. A. Woźniak, M. Owczarek, and S. Drobczyński, "Polarimeter for measuring the properties of birefringent media in reflective mode," Opt. Express **28**(1), 249–257 (2020).

25. M. Sobczak, M. Owczarek, W. A. Woźniak, and P. Kurzynowski, "In vivo measurements of corneal birefringence properties using the one-way reflective Mueller polarimetry," Opt. Express **29**(10), 15356–15365 (2021).

26. M. F. Perutz, "Polarization, dichroism, form birefringence, and molecular orientation in crystalline haemoglobins," Acta Crystallogr. **6**(11), 859–864 (1953).

27. W. L. Bragg and A. B. Pippard, "The form birefringence of macromolecules," Acta Crystallogr. **6**(11), 865–867 (1953).

28. K. M. Meek and C. Knupp, "Corneal structure and transparency," Prog. Retinal Eye Res. **49**, 1–16 (2015).

29. M. Sobczak, M. Asejczyk, K. Kalinowski, and B. Pierścionek, "Comparative analysis of the corneal birefringence pattern in healthy children and adults," Ophthalmic. Physiol. Opt. **41**(4), 715–725 (2021).

30. F. Rüfer, A. Schröder, C. Bader, and C. Erb, "Age-related changes in central and peripheral corneal thickness: determination of normal values with the Orbscan II topography system," Cornea **26**(1), 1–5 (2007).

31. C. Boote, S. Hayes, M. Abahussin, and K. M. Meek, "Mapping collagen organization in the human cornea: left and right eyes are structurally distinct," Invest. Ophthalmol. Visual Sci. **47**(3), 901–908 (2006).

32. S. J. Anthony, "Imaging shear stress distribution and evaluating the stress concentration factor of the human eye," Sci. Rep. **5**(1), 8899 (2015).

33. R. W. Knighton and X. R. Huang, "Linear birefringence of the central human cornea," Invest. Ophthalmol. Visual Sci. **43**(1), 82–86 (2002).

34. S. Fukuda, G. Kishino, S. Hoshi, S. Beheregaray, Y. Ueno, M. Fukuda, D. Kasaragod, Y. Yasuno, and T. Oshika, "Repeatability of corneal phase retardation measurements by polarization-sensitive optical coherence tomography," Invest. Ophthalmol. Visual Sci. **56**(5), 3196–3201 (2015).

35. K. Irsch and A. A. Shah, "Birefringence of the central cornea in children assessed with scanning laser polarimetry," J. Biomed. Opt. **17**(8), 086001 (2012).

36. A. Daxer, K. Misof, B. Grabner, A. Ettle, and P. Fratzl, "Collagen fibrils in the human corneal stroma: structure and aging," Invest. Ophthalmol. Visual Sci. **39**(3), 644–648 (1998).

37. L. Lesueur, J. L. Arne, M. Mignon-Conte, and F. Malecaze, "Structural and ultrastructural changes in the developmental process of premature infants' and children's corneas," Cornea **13**(4), 331–338 (1994).

38. A. Gogola, N.-J. Jan, B. Brazile, P. Lam, K. L. Lathrop, K. C. Chan, and I. A. Sigal, "Spatial patterns and age related changes of the collagen crimp in the human cornea and sclera," Invest. Ophthalmol. Visual Sci. **59**(7), 2987–2998 (2018).

39. K. Hayashi, H. Hayashi, and F. Hayashi, "Topographic analysis of the changes in corneal shape due to aging," Cornea **14**(5), 527–532 (1995).

40. X. Shao, K. J. Zhou, A. P. Pan, X. Y. Cheng, H. X. Cai, J. H. Huang, and A. Y. Yu, "Age-Related Changes in Corneal Astigmatism," J. Refract. Surg. **33**(10), 696–703 (2017).

41. S. Fukuda, M. Yamanari, Y. Lim, S. Hoshi, S. Beheregaray, T. Oshika, and Y. Yoshiaki, "Keratoconus diagnosis using anterior segment polarization-sensitive optical coherence tomography," Invest. Ophthalmol. Visual Sci. **54**(2), 1384–1391 (2013).